726

Structures of Cubic and Orthorhombic Phases of Acetylene by Single-Crystal Neutron Diffraction

By R. K. McMullan and Å. Kvick*

Chemistry Department, Brookhaven National Laboratory, Upton, NY 11973, USA

and P. Popelier†

Department of Chemistry, University of Antwerp (UIA), Universiteitsplein 1, B-2610 Wilrijk, Belgium

Abstract

The crystal structures of acetylene (C_2H_2) at 131 and 141 K and deuteroacetylene (C_2D_2) at 143 and 15 K have been refined by least-squares methods using single-crystal neutron diffraction data. Crystal data: C_2H_2, orthorhombic, $Pa3$, $Z = 4$, $F(000) = 23.26$ fm, $\mu_n = 1.46$ cm^{-1}; $T = 131$, 141 K; $a_o = 6.0940$ (8), 6.1050 (8) Å; $V = 226.31$ (9), 227.54 (9) Å^3, $D_n = 0.7643$ (3), 0.7602 (3) g cm^{-3}, $R(F^2) = 0.065$, 0.052; $wR(F^2) = 0.082$, 0.064; $S = 1.47$, 1.33 for 120, 122 unique reflections [$(\sin\theta/\lambda) \le 0.79$ Å^{-1}] and 8 variable parameters. C_2D_2, $\mu_n = 1.2 \times 10^{-4}$ cm^{-1}, at $T = 143$ K, orthorhombic, $Pa3$, $Z = 4$, $F(000) = 106.58$ fm, $a_o = 6.1020$ (7) Å, $V = 227.20$ (8) Å^3, $D_n = 0.8201$ (3) g cm^{-3}; at $T = 15$ K, cubic, $Acam$, $Z = 4$, $a = 6.198$ (4), $b = 6.023$ (4), $c = 5.578$ (2) Å, $V = 208.2$ (3) Å^3, $D_n = 0.895$ (1) g cm^{-3}. At 143 and 15 K, $R(F^2) = 0.097$, 0.096; $wR(F^2) = 0.068$, 0.081; $S = 1.36$, 1.63 for 120, 119 unique reflections [$(\sin\theta/\lambda) \le 0.79$, 0.74 Å^{-1}] and 8, 14 variable parameters. In the cubic structure, molecules lie at fourfold ($\bar{3}$) positions and exhibit pronounced librational motion about their centers of mass. In the orthorhombic structure, molecules in fourfold ($2/m$) positions are aligned with molecular axes near $\langle 110 \rangle$ directions. At 15 K, notably short intermolecular D$\cdots$C$\equiv$C separations of 2.737 and 2.738 Å within the (001) planes are attributed to weak D-donor to C$\equiv$C π-acceptor interactions. At 131, 141 and 143 K, the observed C—C and C—H(D) bond lengths are strongly affected by thermal motion and are less accurate than the precision indicated by the e.s.d.'s C—C 0.004–0.006, C—H 0.008–0.010 and C—D 0.003 Å. Bond lengths C—C 1.193 (6) and C—D 1.070 (5) Å at 15 K are within 2 e.s.d.'s. of the r_e gas-phase Raman values.

---

* Present address: European Synchrotron Radiation Facility, BP 220–38043, Grenoble CEDEX, France.
† Present address: Department of Chemistry, McMaster University, L8S 4M1 Hamilton, Ontario, Canada.

Introduction

Crystalline acetylene is known to exist in cubic and orthorhombic modifications. The transition temperatures are reported to be 133 K in C_2H_2 (Sugawara & Kanda, 1952) and 149 K in C_2D_2 (Koski & Sándor, 1975a). The structure of cubic C_2H_2 in space group $Pa3$ was determined at 156 K by Sugawara & Kanda (1952) from single-crystal X-ray film data. A more complete analysis was carried out with extensive single-crystal X-ray data measured at 141 K by van Nes & van Bolhuis (1979) as a part of their studies of the electron density distributions in small hydrocarbon molecules. The cubic C_2D_2 structure at 150.5 K has also been refined with neutron powder data (Koski, 1975a), but the analysis provided structural parameters of lower accuracy than required for the electron density study (van Nes & van Bolhuis, 1979). At temperatures above the phase transition, large-amplitude thermal displacements of the acetylene molecules severely limit the accuracy attainable by crystal structure analyses. The low-temperature phase was observed by X-ray diffraction (Sugawara & Kanda, 1952) and by solid-state IR (Bottger & Eggers, 1964; Anderson & Smith, 1966; Smith, 1969); its crystal structure was first correctly described with symmetry D_{2h}^{18} from analysis of solid-state Raman data at 4.2 and 77 K (Ito, Yokoyama & Suzuki, 1970). Structural parameters were determined from neutron powder data on C_2D_2 at 4.2 K in space group $Acam$ (Koski & Sándor, 1975b; Koski, 1975b) and also refined at 77 and 109 K (Koski, 1975c,d) against neutron powder data. Attempts to measure reliable single-crystal X-ray intensity data (van Nes & van Bolhuis, 1979) were frustrated by the poor quality of crystals obtained on phase transformation.

In the present work, we report refinements against single-crystal neutron diffraction data for cubic C_2H_2 and C_2D_2 aimed at improving our description of the thermal vibrations and packing configurations of

molecules in solid acetylene. We also report a refinement for orthorhombic C_2D_2 against neutron diffraction data measured at 15 K with a single-crystal fragment obtained by phase transformation. The structural parameters derived for the cubic phase provide experimental values for comparison with theoretical results obtained for solid C_2H_2 and C_2D_2 by crystal-field *ab initio* methods (Lenstra, van Alsenoy, Popelier & Geise, 1992).

Experimental

Sample preparation

Single crystals were grown from gaseous C_2H_2 and C_2D_2 inside a cryostat (Air Products & Chemical, Inc., Displex® Model CS-202) on the H6M four-circle diffractometer at Brookhaven National Laboratory. Gas samples of C_2H_2 (Matheson Chemical Company) and C_2D_2 (Cambridge Isotope Laboratories) were each condensed with liquid nitrogen in a vacuum line, residual gases were removed, and the acetylene gases were introduced into sample bulbs fitted with Pt insert pins as sites for crystal nucleation (Kvick, McMullan & Newton, 1982). The initial P, V, T gas parameters (30.9 KPa, 9 cm^3, 295 K) were chosen to obtain crystals of ~4mm^3 volume, based on calculated crystal densities. Crystal growth on the diffractometer was controlled by heat conduction along the Pt pin attached to the cryostat, which provided stability < 0.1 K. Approximately 70% of each sample was condensed as the cubic phase at 160 K (vapor pressure, 7.3 KPa). Intense reflections of forms {200} (C_2H_2) and {111} (C_2D_2) were monitored to determine the number of crystals present and their relative sizes and growth rates. Repeated heating and cooling between 155 ± 10 K served to induce growth of the major crystals at the expense of the smaller crystals initially formed. The crystals showed good diffraction characteristics with Gaussian scan profiles and full-widths at half-heights < 0.35° in angle ω. Cooling the crystals through the phase transitions at rates < 0.1° min^{-1} produced abrupt and irreversible intensity losses in the monitor reflections at 127 K (C_2H_2) and 139 K (C_2D_2). Scans in ω showed that the crystals fragmented during phase transformations.

For intensity measurements, the cubic C_2H_2 and C_2D_2 crystals were prepared from gaseous samples as described above; the orthorhombic C_2D_2 crystal was grown during ~12 h at 131 K from the largest fragment of a transformed cubic crystal. Searches on angles χ and φ revealed the presence of crystallites in each sample, a second crystal in the cubic C_2D_2 sample, and several crystal fragments in the orthorhombic sample. Reflection-angle settings of the largest crystals in each sample were recorded. The orientation matrices, determined from the consistent

subsets of angle settings, were used to indentify satellite-crystal reflections that could affect intensities of the primary crystals.

Diffraction data

The experimental conditions used in the intensity measurements are summarized in Table 1. The neutron beam, monochromated by reflection from Be(002) planes, was of wavelength 1.0402 (1) Å based on KBr ($a_o = 6.0000$ Å at 298 K). For each acetylene sample, the primary crystal was centered precisely in the neutron beam, as previously described (Kvick et al., 1982). The unit-cell parameters were determined by least-squares fits of $\sin^2\theta$ values for 30 reflections with $40 < 2\theta < 52°$. In the cubic phases, reflection intensities were collected within one quadrant, $(h \pm kl; h, |k|, l \le 9)$ for C_2H_2 and $(h \bar{k} \pm l; h, |k|, |l| \le 9)$ for C_2D_2; in the orthorhombic phase, the data were collected within the hemisphere $(\pm h k \pm l; |h|, k \le 9, |l| \le 8)$. The intensities were measured by the $\omega/2\theta$ step-scan method, using the 2θ scan ranges defined in Table 1; $\Delta 2\theta$ step intervals adjusted to count 65–85 points per scan; and the accumulated counts per point limited by preset monitor counts of the direct beam, requiring ~2 s. The intensities of two reference reflections were monitored after every 50 reflections; no significant variations were noted during collection of the data sets. The space-group extinction rules for $Pa3$ and $Acam$ were verified at 131 and 15 K. Apparent violations observed up to $6\sigma(I)$ were all attributable to intensity contributions from satellite crystals or from Pt and Al powder lines recorded on 2θ scans. The integrated intensity I_i for each reflection was obtained by subtracting the background as estimated from the two outer 10% parts of the scan. Variances $\sigma_c^2(I_i)$ were derived from counting statistics. No corrections were applied for neutron absorption by the crystals.* Symmetry-equivalent F_{oi}^2 ($= I_i \sin 2\theta$) values were averaged with weights, $w_i = \sigma_c^{-2}(I_i)$, giving the internal agreement indices listed in Table 1. An observation with $|I_i - \bar{I}| > 4\sigma_c(I_i)$ was omitted in averaging if there then remained three or more non-disparate values. The variance $\sigma^2(F_o^2)$ in the average $\bar{F_o}^2$ value of equivalent reflections was assigned as $\{[\sigma_c^2(F_{oi}^2)]_{av} + (1/N - 1)\Sigma|F_{oi}^2 - \bar{F_o}^2|^2\}$, where the first term is the average variance from counting statistics and second is the dispersion from the $\bar{F_o}^2$ value. The reflections affected by Pt and Al powder intensities (10 cubic and 30 orthorhombic reflections) were deleted from the independent data sets (Table 1) used in the refinements.

---

* The linear absorption coefficients μ are 1.2×10^{-4} cm^{-1} for C_2D_2 and 1.456 cm^{-1} for C_2H_2 at $\lambda = 1.0402$ Å, as evaluated from μ/ρ values for hydrogen (Koetzle & McMullan, 1980), deuterium and carbon (*International Tables for X-ray Crystallography*, 1962, Vol. III).

Table 1. *Crystallographic data and structure refinement*

	C_2H_2	C_2H_2	C_2D_2	C_2D_2
Temperature[a] (K)	131	141	143	15
Space group	$Pa3$	$Pa3$	$Pa3$	$Acam$
Lattice parameters (Å)				
a	6.0940 (8)	6.1050 (8)	6.1020 (7)	6.198 (4)
b				6.023 (4)
c				5.578 (2)
Cell volume (Å³)	226.31 (9)	227.54 (9)	227.20 (8)	208.2 (3)
Density (g cm⁻³)	0.7643 (3)	0.7602 (3)	0.8201 (3)	0.895 (1)
Intensity measurements				
$(\sin\theta/\lambda)_{max}$ (Å⁻¹)	0.79	0.79	0.79	0.74
Scan range $2\theta = a + b\tan\theta$				
a; b (°) (0 < 2θ < 55°)	3.0; 0.0	3.0; 0.0	3.0; 0.0	3.6; 0.0
a; b (°) (55 < 2θ < 108°)	1.94; 2.25	1.94; 2.25	1.94; 2.25	1.43; 4.49
Intensity standards	304, 043	304, 043	4̄30, 3̄04	4̄31, 4̄31
Number of observations				
Total[b]	1024	867	887	827
Independent	154	155	155	175
Internal agreement[c]	0.070	0.082	0.098	0.084
Refinement				
Number of observations, n	120	122	120	119
Number of variables, v	8	8	8	14
Indices of fit[d]				
$R(F^2)$	0.065	0.082	0.097	0.096
$wR(F^2)$	0.052	0.064	0.068	0.081
S	1.470	1.327	1.357	1.632

Notes: (a) The transition $Pa3 \longleftrightarrow Acam$ is at 127 K (C_2H_2) and 139 K (C_2D_2) as recorded by the sensor in the cryostat cold tip holding the Pt pin and crystal. (b) Recorded in six equivalent reciprocal lattice sectors at 141, 131, 143 K and four equivalent sectors at 15 K, with space-group absences included at 131 and 15 K. (c) $\Sigma w|F_i^2 - \bar{F}^2|/\Sigma w\bar{F}^2$. (d) $R(F^2) = \Sigma F_o^2 - F_c^2 /\Sigma F_o^2$; $wR(F^2) = [\Sigma w|F_o^2 - F_c^2|^2/\Sigma(wF_o^2)^2]^{1/2}$; $S = [\Sigma w|F_o^2 - F_c^2|^2/(n - v)]^{1/2}$.

Structure refinements

Initial nuclear positions for refinements of the cubic and orthorhombic structures were taken from van Nes & van Bolhuis (1979) and Koski (1975b), respectively. The refinements were carried out with the full-matrix least-squares program of Lundgren (1982). The residuals $\Sigma w|F_o^2 - F_c^2|^2$ were minimized with weights $w = \sigma^{-2}(F_o^2)$, summing over the independent reflections with $F_o^2 > -\sigma(F_o^2)$. The neutron-scattering amplitudes (fm) (6.6484 for C; -3.7409 for H; 6.674 for D) were taken from the tabulation of Koester (1977). In each refinement, the variable parameters were the free coordinates and anisotropic thermal parameters, one scale factor, and the isotropic secondary-extinction parameter for a type-I crystal with Lorentzian mosaic spread (Becker & Coppens, 1974). Uniform mean crystal path lengths were assumed for estimating extinction effects by parameter refinement. Extinction corrections greater than 10% were obtained for three cubic reflections and one orthorhombic reflection, the largest of these ($\times F_o^2$) being for reflections (200) (1.54 at 141 K), (111) (1.46 at 143 K) and (002) (1.20 at 15 K). The deuterium scattering amplitudes were varied to test the isotopic purity of C_2D_2; the refined values agreed with 6.674 fm (above) within 0.8σ (143 K) and 1.1σ (15 K), and were fixed at 6.674 fm in the final refinements. The parameter shifts at convergence were all $< 0.01\sigma$. In the final difference maps, the largest residuals $|\Delta\rho|$, as %ρ of carbon in ρ_{obs} maps, were 4.6, 5.2, 5.1 and 3.5% at 141, 131,

143 and 15 K respectively. These were located at special positions ($\frac{1}{2}$, 0, 0, etc.) in the 141 and 143 K maps, near hydrogen positions in the 131 K map, and were without special significance in the 15 K map. The final nuclear positional and anisotropic thermal parameters are listed in Table 2.*

Results and discussion

The phase transformations (Table 1) were observed at 6 and 10 K below transition temperatures T_c determined, respectively, by X-ray diffraction for C_2H_2 (Sugawara & Kanda, 1952; van Nes & van Bolhuis, 1979) and by powder neutron diffraction for C_2D_2 (Koski & Sándor, 1975a). We are not aware of any thermodynamic measurements of T_c for either C_2H_2 or C_2D_2. In the present study, the observed differences in T_c may indicate temperature gradients of 10 ± 2K between the sensor-to-sample positions. Comparable uncertainties in measurement temperatures appear evident among the independently determined lattice constant a_o of the cubic phase (Fig. 1).

Stereoviews of the packing arrangements in cubic and orthorhombic C_2D_2 are provided in Fig. 2 for comparison. The molecules in the cubic structure are

Table 2. *Nuclear positional and thermal parameters*

Anisotropic thermal factors ($\times 10^3$) have the form:
$$\exp(-2\pi^2 \Sigma_i \Sigma_j h_i h_j a_i^* a_j^* U_{ij}).$$

Cubic	C_2H_2 (131 K)	C_2H_2 (141 K)	C_2D_2 (143 K)
C x	0.0562 (2)	0.0556 (3)	0.0538 (2)
C U_{11}	57.3 (8)	61.8 (9)	60.4 (13)
C U_{12}	−1.1 (7)	−0.9 (8)	−6.7 (9)
H(D) x	0.1524 (6)	0.1525 (7)	0.1519 (4)
H(D) U_{11}	130.5 (19)	139.9 (27)	141.3 (24)
H(D) U_{12}	−33.0 (19)	−37.5 (21)	−40.7 (16)
Orthorhombic C_2D_2 (15 K)			
C x, y, z	0.0621 (5)	0.0756 (5)	0.0000
C U_{11}, U_{22}, U_{33}	17.8 (9)	16.3 (9)	27.2 (13)
C U_{12}, U_{13}, U_{23}	−2.0 (11)	0.0	0.0
D x, y, z	0.1709 (6)	0.2135 (6)	0.0000
D U_{11}, U_{22}, U_{33}	44.9 (23)	32.2 (18)	57.0 (22)
D U_{12}, U_{13}, U_{23}	−14.4 (17)	0.0	0.0

located at fourfold positions of $\bar{3}$ symmetry in *Pa*3, with average bond directions along threefold axes, as in the CO_2 structure (Wyckoff, 1963). In the orthorhombic structure, molecules lie in the mirror planes of *Acam* at fourfold positions of $2/m$ symmetry with molecular axes aligned approximately along $\langle 110 \rangle$ directions, as in solid chlorine (Collins, 1952). The transformation *Pa*3 → *Acam* from the three-dimensional to the layer structure (Fig. 3) involves rotations of molecules by ~35°, from directions $\langle 111 \rangle$ to $\langle 110 \rangle$, and relative displacements of alternate layers by $\frac{1}{2}[110]$. The resulting large anisotropic changes in cell metrics (*cf.* Table 1) probably induce strains that cause the observed loss of crystal integrity. In both structures, each molecule has an environment of six neighbors at internuclear distances less than 3.6 Å. In the more loosely packed
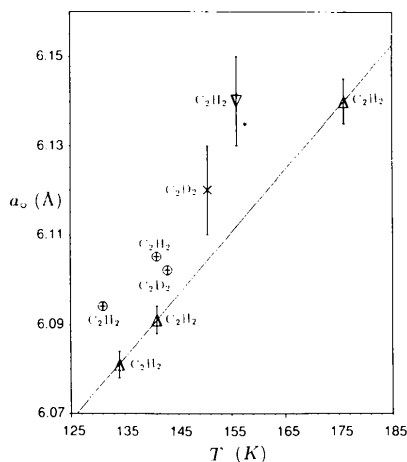

Fig. 1. Cubic acetylene. Lattice constant a_o (Å) *versus* temperature (K). References sources are given by symbols △ (van Nes & van Bolhuis, 1979), ⊕ (Table 1), × (Koski, 1975a), ▽ (Sugawara & Kanda, 1952). Points on the line (△) are reported with reference to T_c of 133 K for C_2H_2. The minimum differences between the line and disparate values are: 10 ± 2K (⊕), 7.5 K (×), 16 K (▽).

cubic arrangement, the shortest distances (Table 3*b*), exceed the sums of van der Waals radii 2.4 and 2.9 Å, [r(H) = 1.2, r(C) = 1.7 Å; Pauling, 1960] and are invariant within ± 0.004 Å (2σ) over the limited range of 131–143 K. Although the layer structure provides denser packing, there are no unusally close contacts between atoms of adjacent layers, the shortest being C···C and D···D distances at 3.575 and 2.956 Å. The shortest and more interesting interactions occur within layers, as shown in Fig. 3. Each molecule is confined between four others at C···D distances of 2.737 (5) and 2.738 (5) Å that are ~0.2 Å shorter than expected van der Waals separations. The two distinct distances at 4.2 K are given as 2.73 (2) Å by Koski & Sándor (1975*b*). Within the present experimental uncertainty, the molecular long axis points directly at carbon atoms of two adjacent molecules, while the molecular center lies midway between deuterons of two other molecules at a distance of 2.672 Å. The $(C_2D_2)_2$ groups of this array have the T-shaped geometry described as the configuration for the hydrogen-bonded C_2H_2.HF complex from gas-phase microwave (Read & Flygare, 1982), electric dipole moment (Nelson, Fraser & Klemperer, 1985) and IR (Huang & Miller, 1987) studies. This geometry is clearly optimal for donor–acceptor interactions involving the deuterons and triple-bond π electrons. The C≡C···D distance is longer in solid acetylene than in the gas-phase complex (2.67 *versus* 2.19 Å; Read & Flygare, 1982), and the bonding weaker, consistent with the donor acetylene molecule being more weakly acidic than HF. In crystalline diiodoacetylene, a similar but somewhat less favorable geometry has been observed by Dunitz, Gehrer & Britton (1972) who described the C≡C···I interactions as donor–acceptor-type bonding. In acetylene, the extensive cross-linking of molecules with these weak interactions appears to be a major factor contributing to the stability of the low-temperature phase.

The bond lengths of C_2H_2 and C_2D_2 from gas-phase Raman and diffraction measurements are listed in Table 3(*a*) at nominal temperatures reported by the authors. This tabulation illustrates well the difficulty attendant to obtaining precise and accurate bond lengths for the acetylene molecule from diffraction data for the cubic phase. The bond lengths derived for the two structures in this study are of comparable precision, despite the 15 K diffraction data being lower in resolution and more affected by random contributions from satellite crystals. At 15 K the C—C and C—D lengths differ by less than 2σ from either the equilibrium gas phase or the 4.2 K neutron powder values (Table 3*a*). The C—C—D angle of 178.9 (5)°, unconstrained by symmetry in *Acam*, is consistent with a linear molecule within 2σ. The C—H(D) bond lengths, corrected for effects of

thermal motion by the Busing & Levy (1964) riding model, are 1.10, 1.12, 1.14, 1.15 Å (15, 131, 141, 143 K); corresponding 'minimum' values for correlated parallel displacements of C and H(D) are 1.08, 1.04, 1.05, 1.06 Å. The unusually large values for thermal-motion parameters U_{ij} of the cubic structure (Fig. 2a, Table 2) are attributed mainly to rigid-body librational motion about the molecular centers of mass. Table 4 lists the mean-square amplitudes of atomic vibrations computed from the rectilinear displacement parameters U_{ij} (Table 2), in directions
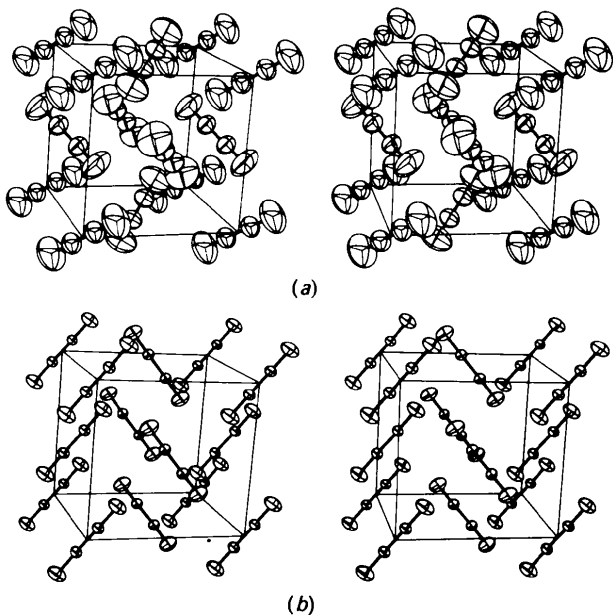

(a)

(b)

Fig. 2. Stereoviews of C_2D_2 molecules in the cubic structure (a) at 143 K and in the orthorhombic structure (b) at 15 K, approximately down the c axis with the a axis horizontal. Planes of molecules in (b) are separated by $\frac{1}{2}c$. Thermal-ellipsoid surfaces are at 50% probability levels (Johnson, 1976). ORTEP diagrams for cubic C_2H_2 at 131 and 141 K do not differ perceptibly from (a).
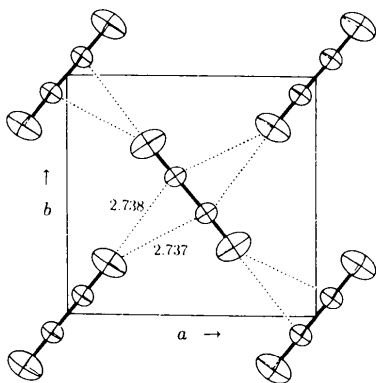

Fig. 3. Arrangement of C_2D_2 molecules on the orthorhombic (001) face at 15 K, showing the shortest intermolecular separations in Å. Thermal-ellipsoid surfaces are at 75% probability levels.

Table 3. *Bond-length (Å) measurements and intermolecular distances (Å) less than 3.6 Å for C_2H_2 and C_2D_2, uncorrected for thermal vibration effects*

Bond lengths

	C—C	C—H(D)	Temp. (K)	Structure
C_2H_2 and C_2D_2	1.2033 ± 2	1.0605 ± 3		Gas[a]
C_2H_2	1.20 (2)	1.05 (5)	156	Pa3[b]
C_2D_2	1.15 (1)	1.06 (1)	150.5	Pa3[c]
C_2D_2	1.138 (5)	1.036 (3)	143	Pa3[d]
C_2H_2	1.178 (2)	1.043	141	Pa3[e]
C_2H_2	1.177 (6)	1.024 (10)	141	Pa3[d]
C_2H_2	1.186 (4)	1.016 (8)	131	Pa3[d]
C_2D_2	1.193 (6)	1.070 (5)	15	Acam[d]
C_2D_2	1.180 (6)	1.061 (5)	4.2	Acam[f]

Notes: (a) Raman, gas phase (Fast & Welsh, 1972); equilibrium r_e (C—C) and r_e (C—D) values. (b) X-ray, single crystal (Sugawara & Kanda, 1952). (c) Neutron, powder (Koski, 1975b). (d) Neutron, single crystal (present work). (e) X-ray, single crystal (van Nes & van Bolhuis, 1979); C—H distance constrained. (f) Neutron, powder (Koski, 1975b).

Intermolecular distances

	15 K	131 K	141 K	143 K
C···H(D)	2.737 (5)[i]	3.091 (4)[i]	3.095 (5)[i]	3.098 (4)[i]
	2.738 (5)[ii]	3.290 (4)[ii]	3.293 (5)[ii]	3.289 (4)[ii]
	3.348 (3)[iii]			
	3.388 (2)[iv]			
H(D)···H(D)	2.956 (3)[iii]	3.271 (3)[i]	3.276 (3)[i]	3.278 (3)[i]
	3.130 (2)[i]			
	3.167 (3)[ii]			
C···C	3.575 (4)[iv]			

Symmetry codes: *Acam* (i) $\frac{1}{2}+x$, $\frac{1}{2}-y$, z; (ii) $\frac{1}{2}-x$, $\frac{1}{2}+y$, $-z$; (iii) $\frac{1}{2}-x$, y, $\frac{1}{2}-z$; (iv) $-x$, $\frac{1}{2}-y$, $\frac{1}{2}-z$. *Pa3* (i) $\frac{1}{2}-x$, $-\frac{1}{2}+y$, z; (ii) $-\frac{1}{2}+x$, $\frac{1}{2}-y$, $-z$.

parallel $U_{||}$ and transverse $U_\perp$ to the molecular axes of C_2H_2 at 131 and 141 K and C_2D_2 at 143 and 15 K. Rigid-bond tests (Hirshfeld, 1976) with differences $[U(H,D) - U(C)]_{||}$ give mean-square amplitudes for stretching vibrations of 0.010 (5) (131 K), 0.005 (4) Å² (141 K) for C—H and 0.013 (3) (143 K), 0.008 (2) Å² (15 K) for C—D, indicating that only those for C—D are significant above the experimental 2σ level. It is of interest to compare the $U_{||}$ and $U_\perp$ amplitudes (Table 4) with those derived from the charge density X-ray refinement of cubic C_2H_2 (van Nes & van Bolhuis, 1979). In that study, the hydrogen vibrational amplitudes for the refinement models were obtained from variable carbon $U_{||}$ and $U_\perp$ parameters assuming rigid-body motion with contributions from internal vibrations. The values of $U_{||}$ and $U_\perp$, obtained by van Nes & van Bolhuis (1979) in spherical-atom refinement C1 (their Table 5), 55.8 (10), 52.6 (8) Å² × 10³ for carbon and 63.0, 168.3 Å² × 10³ for hydrogen, are in good agreement with our values at 131 K (Table 4). Values from aspherical refinements were generally in poorer accord and indicated greater thermal anisotropy than the neutron values in Table 4. Larger thermal-vibrational amplitudes obtained in X-ray refinements may be attributed to difficulties in deconvoluting effects of pronounced thermal motion and charge-density distributions.

Table 4. *Mean-square amplitudes of nuclear displacements* ($\text{Å}^2 \times 10^3$) *parallel* $U_{\parallel}$ *and transverse* $U_{\perp}$ *to* C—H *and* C—D *bond directions*

	C_2H_2 (131 K)	C_2H_2 (141 K)	C_2D_2 (143 K)	C_2D_2 (15 K)
C U	55 (2)	60 (2)	47 (2)	15 (1)
C $U_{\perp}$	59 (1)	63 (1)	67 (2)	19 (1), 27 (1)*
H(D) U	65 (4)	65 (4)	60 (2)	23 (2)
H(D) $U_{\perp}$	163 (2)	177 (4)	182 (4)	54 (3), 57 (2)*

* Normal to layers of molecules ($= U_{33}$).

References

ANDERSON, A. & SMITH, W. H. (1966). *J. Chem. Phys.* **44**, 4216–4219.
BECKER, P. J. & COPPENS, P. (1974). *Acta Cryst.* A30, 129–147.
BOTTGER, G. L. & EGGERS, D. F. (1964). *J. Chem. Phys.* **40**, 2010–2017.
BUSING, W. R. & LEVY, H. A. (1964). *Acta Cryst.* **17**, 142–146.
COLLINS, R. L. (1952). *Acta Cryst.* **5**, 431–432.
DUNITZ, J. D., GEHRER, H. & BRITTON, D. (1972). *Acta Cryst.* A28, 1899–1994.
FAST, H. & WELSH, H. L. (1972). *J. Mol. Spectrosc.* **41**, 203–221.
HIRSHFELD, F. L. (1976). *Acta Cryst.* A32, 239–244.

HUANG, Z. S. & MILLER, R. E. (1987). *J. Chem. Phys.* **86**, 6059–6064.
ITO, M., YOKOYAMA, T. & SUZUKI, M. (1970). *Spectrochim. Acta,* **26A**, 695–705.
JOHNSON, C. K. (1976). *ORTEPII.* Report ORNL-5138. Oak Ridge National Laboratory, Tennessee, USA.
KOESTER, L. (1977). *Springer Tracts in Modern Physics,* Vol. 80, *Neutron Physics,* edited by G. HÖHLER, p. 36. Berlin: Springer.
KOETZLE, T. F. & MCMULLAN, R. K. (1980). Research Memo C-4. Brookhaven National Laboratory, USA.
KOSKI, H. K. (1975a). *Z. Naturforsch. Teil A,* **30**, 1028–1031.
KOSKI, H. K. (1975b). *Acta Cryst.* B31, 933–935.
KOSKI, H. K. (1975c). *Cryst. Struct. Commum.* **4**, 337–341.
KOSKI, H. K. (1975d). *Cryst. Struct. Commum.* **4**, 343–347.
KOSKI, H. K. & SÁNDOR, E. (1975a). *Chem. Phys. Lett.* **30**, 501–503.
KOSKI, H. K. & SÁNDOR, E. (1975b). *Acta Cryst.* B31, 350–353.
KVICK, Å., MCMULLAN, R. K. & NEWTON, M. D. (1982). *J. Chem. Phys.* **76**, 3754–3761.
LENSTRA, A. T. H., VAN ALSENOY, C., POPELIER, P. & GEISE, H. J. (1992). To be published.
LUNDGREN, J.-O. (1982). Report UUIC-B13-4-05. Institute of Chemistry, Univ. of Uppsala, Sweden.
NELSON, D. D., FRASER, G. T. & KLEMPERER, W. (1985). *J. Chem. Phys.* **82**, 4483–4485.
NES, G. J. H. VAN & VAN BOLHUIS, F. (1979). *Acta Cryst.* B35, 2580–2593.
PAULING, L. (1960). *The Nature of the Chemical Bond,* 3rd ed. Ithaca: Cornell Univ. Press.
READ, W. G. & FLYGARE, W. H. (1982). *J. Chem. Phys.* **76**, 2238–2246.
SMITH, W. H. (1969). *Chem. Phys. Lett.* **3**, 464–466.
SUGAWARA, T. & KANDA, E. (1952). *Sci. Rep. Res. Inst. Tôhoku Univ. Ser. A,* **4**, 607–614, as quoted by VAN NES & VAN BOLHUIS (1979).
WYCKOFF, R. W. G. (1963). *Crystal Structures,* 2nd ed., Vol. 1, p. 368. New York: Interscience.

---

meso- and D,L-D_3-Trishomocubylidene-D_3-trishomocubane Oxides and D,L-Bi-D_3-trishomocubyl

BY WILLIAM H. WATSON,* RAM P. KASHYAP AND MARIUSZ KRAWIEC

Department of Chemistry, Texas Christian University, Fort Worth, Texas 76129, USA

AND ALAN P. MARCHAND,* C. MADHUSUDHAN REDDY AND VIJAY R. GADGIL

Department of Chemistry, University of North Texas, PO Box 5068, Denton, Texas 76203, USA

Abstract

meso-D_3-Trishomocubylidene-D_3-trishomocubane oxide, (2a), $C_{22}H_{24}O$, $M_r = 304.44$, monoclinic, $P2_1/a$, $a = 12.337$ (2), $b = 6.361$ (3), $c = 19.891$ (2) Å, $\beta = 96.44$ (1)°, $V = 1551.1$ (9) Å³, $Z = 4$, $D_x = 1.303$ g cm⁻³, λ(Mo $K\alpha$) = 0.71069 Å, $\mu = 0.72$ cm⁻¹, $F(000) = 656$, $T = 296$ K, $R = 0.049$ for 1321 reflections. D,L-D_3-Trishomocubylidene-D_3-trishomocubane oxide, (2b), $C_{22}H_{24}O$, $M_r = 304.44$, monoclinic, $C2/c$, $a = 21.471$ (5), $b = 6.352$ (1), $c = 12.351$ (3) Å, $\beta = 117.26$ (1)°, $V = 1497.4$ (6) Å³, $Z = 4$, $D_x = 1.350$ g cm⁻³, λ(Cu $K\alpha$) = 1.54178 Å, $\mu = 5.77$ cm⁻¹, $F(000) = 656$, $T = 296$ K, $R = 0.051$ for 1085 reflections. D,L-Bi-D_3-trishomocubyl, (3), $C_{22}H_{26}$, $M_r = 290.45$, triclinic, $P\bar{1}$, $a = 6.324$ (1), $b = 10.591$ (2), $c = 11.767$ (3) Å, $\alpha = 103.14$ (2), $\beta = $